

# Hierarchical Organizations

IM

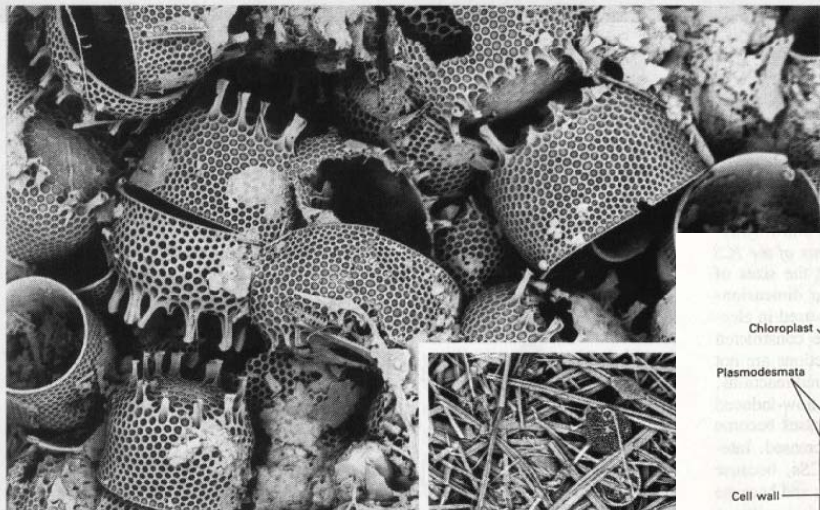
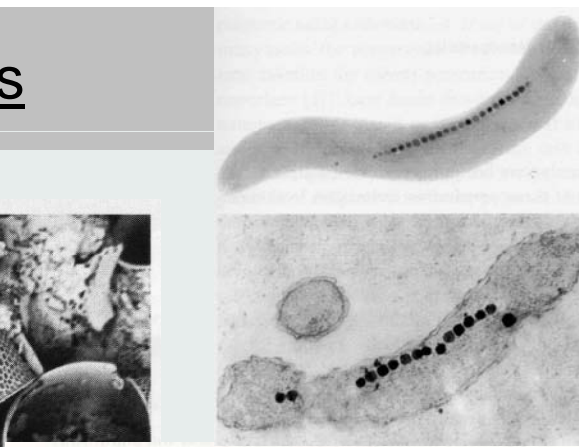


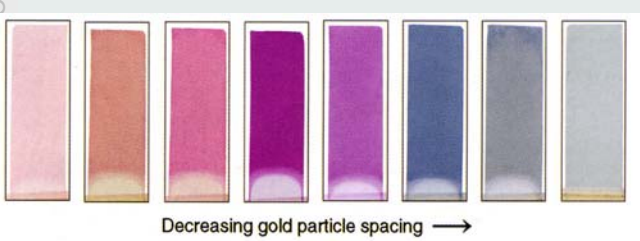
Figure 1 Evidence of the 'fall dump' of giant diatoms identified by Kemp *et al.*<sup>1</sup>. Above, a sediment layer from the Gulf of California dominated by cell walls of *Stephanopyxis palmeriana* (diameter < 70 µm). Right, a sediment layer from the Southern Ocean, showing a tangled mass of the rod-shaped species *Thalassiothrix antarctica*, which grows up to 4 mm in length. (Courtesy of A. E. S. Kemp.)



## Metals NPs in Solutions and in Polymers

P. Mulvaney, MRS Bull. 2001, 26, 1009

R. NESPER ETH ZÜRICH & CO. I ECCLIM LIUVIETICUM



$$R = \frac{(n - 1)^2 + k^2}{(n + 1)^2 + k^2},$$

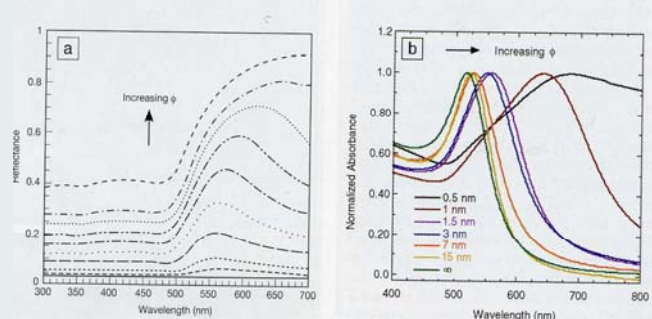
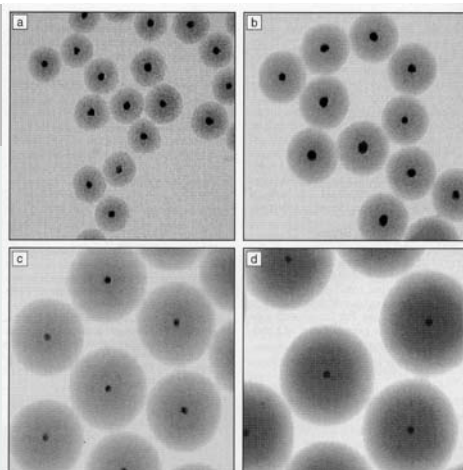
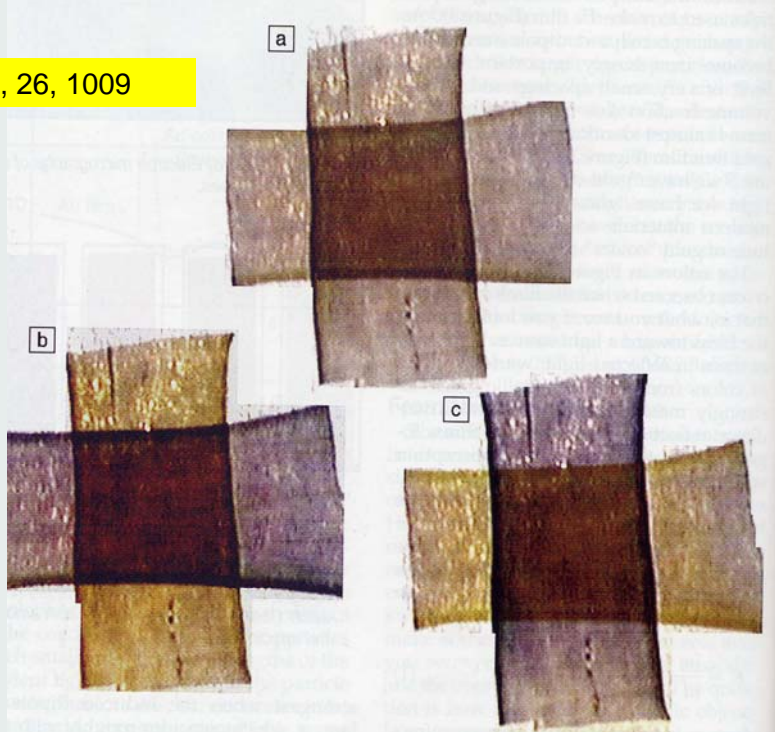


Figure 5. The transmitted colors of a series of gold particle films with decreasing particle spacing. The gold core particles are 15 nm in diameter; the shell thicknesses are, from left to right, 17.5 nm, 12.5 nm, 4.6 nm, 2.9 nm, 1.5 nm, 1.0 nm, 0.5 nm and 0 nm. Films are each 1 cm × 3 cm. The spectra shift smoothly between the two curves shown in Figure 3 as the spacing is varied.<sup>9</sup>

Figure 6. (a) Normalized reflectance spectra for Au@SiO<sub>2</sub> (gold concentrically coated by silica) films as a function of the volume fraction  $\phi$  of Au. From the bottom curve upward,  $\phi$  for each curve, respectively, is 0.01, 0.05, 0.10, 0.20, 0.30, 0.40, 0.50, 0.60, 0.70, and pure Au. (b) The normalized absorbance of a series of Au@SiO<sub>2</sub> films as a function of particle spacing.

# Metals NPs in Solutions and in Polymers

P. Mulvaney, MRS Bull. 2001, 26, 1009



29.10.2008

Figure 7. Photographs of aligned Ag nanorods in a poly(vinyl alcohol) film. The images shown are the transmitted colors with (a) unpolarized light, (b) horizontally polarized light, and (c) vertically polarized light.

# Fullerenes in CNTs

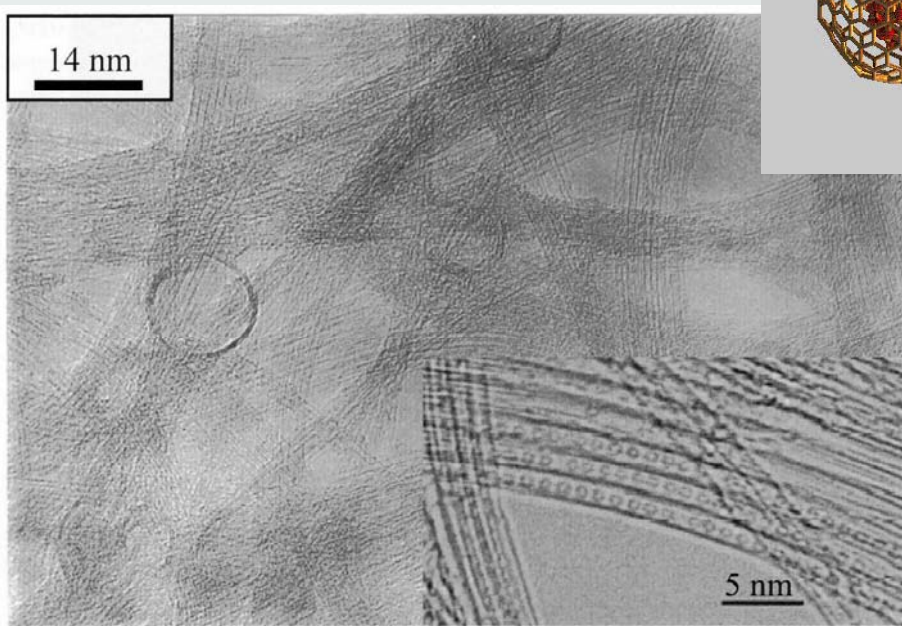
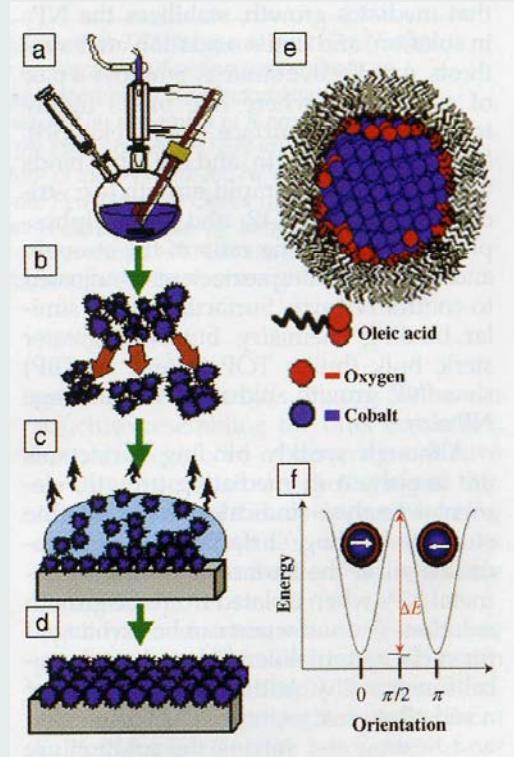


Fig. 8.6. HREM image of SWNTs obtained by arcing graphite electrodes filled with Ni and  $\text{Y}_2\text{O}_3$  under a He atmosphere (660 Torr). Inset: The HREM image of encapsulated fullerenes inside the SWNTs; scale bar is 5 nm. Reproduced from ref. [45], with permission.

# Selforganization of Magnet Colloids



29.10.2008

Nanochemistry UIO

5

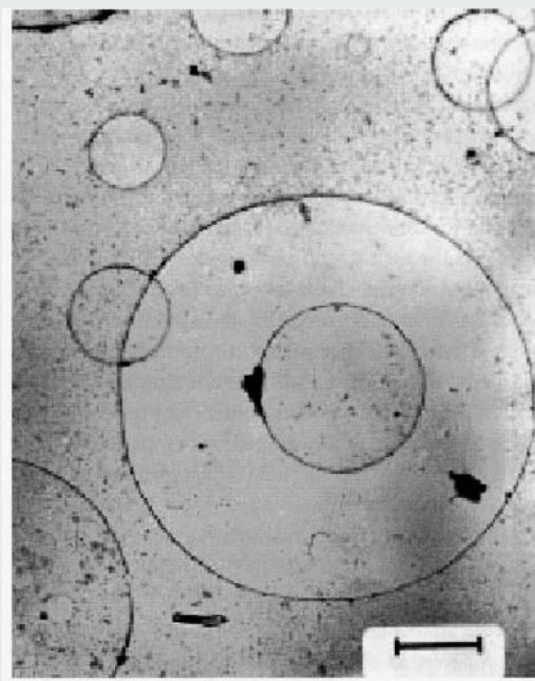
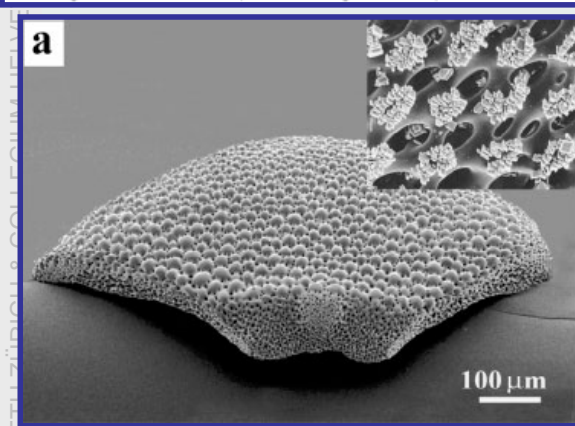


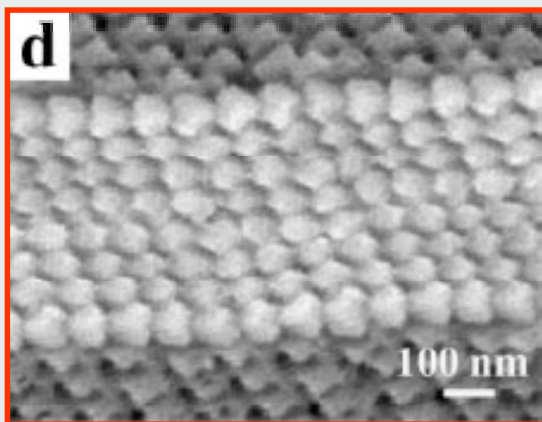
Fig. 6.4. TEM micrograph showing the self-organization of super-paramagnetic nanoparticles into submicron size rings the so-called *Olympic Rings* (scale bar is 0.7  $\mu\text{m}$ ).

# Hierarchical Crystals from Biomin

Figure 1. Scanning electron micrographs of biogenic calcium carbonate structures: a) Dorsal arm plate of the brittle star *Ophiocoma wendti* with the external array of microlenses. The entire elaborate structure is a single calcite crystal. The lenses are oriented in the optic axis direction of the constituent birefringent calcite. Inset: Epitaxial overgrowth of synthetic calcite crystals on a brittlestar stereom. Note that the nucleation of the newly formed calcite



Adv. Mater. 2004, 16, No. 15,



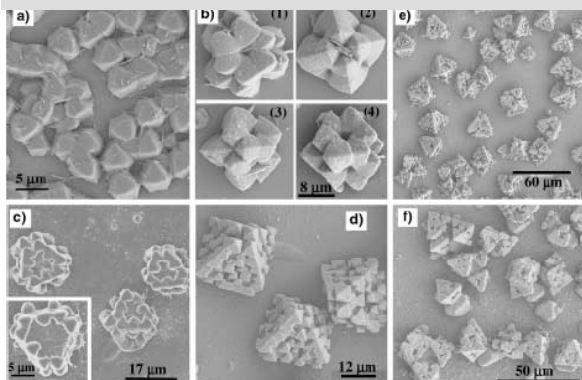
and macromolecules to the local sites of active growth (indicated by arrows). d) Fragment of a coccolith skeleton composed of a highly periodic array of oriented, uniform nanocrystals of calcite.

29.10.2008

Nanochemistry UIO

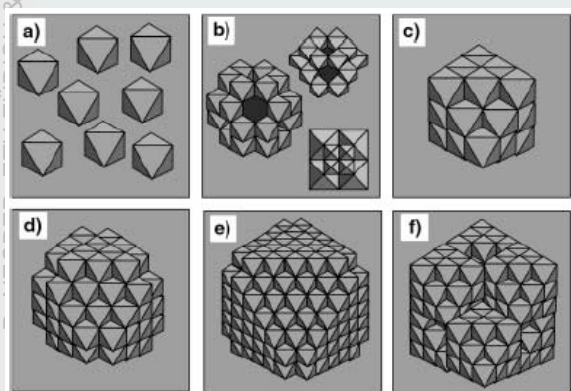
6

# Super Crystals



hybrid mesoporous crystals using 1,2-bis(trimethoxy silyl) ethane (BTME) as a silica source and Hexadecyl-trimethylammonium chloride (CTAC) as a surfactant

*Angew. Chem. Int. Ed.* 2003, 42, 413



Schematic illustrations of edge-sharing stacking:  
 a) primary octahedral units, face-on configurations,  
 b) quartet-octahedron model for the secondary structure,  
 c) tertiary structure with filled corners,  
 d) tertiary structure with unfilled corners,  
 e) a high-order structure from primary octahedra,  
 f) a high-order structure from tertiary units.

29.10.2008

Nanochemistry UIO

7

## Principal Forms of Hierarchical Organization

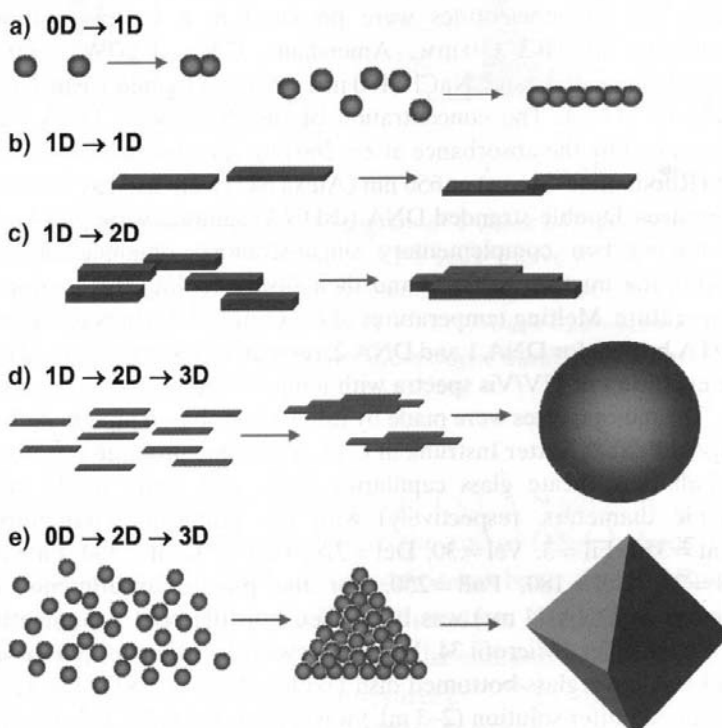


**Figure 1.** Various organizing schemes for self-construction of nano-structures by oriented attachment.

29.10.2008

Nanochemistry UIO

8

# Metal Cluster Organizations

R. NESPER ETH ZÜRICH & COLLEGIUM HELVETICUM

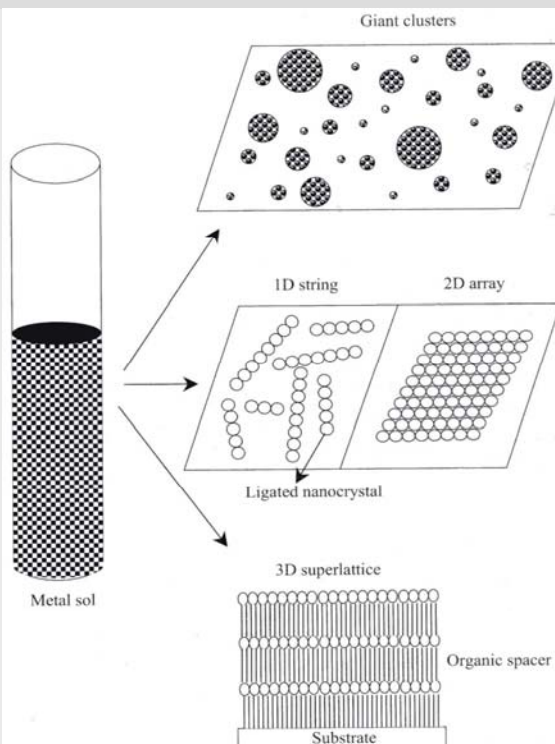


Fig. 4.8. Schematic illustration of the various metal nanocrystal organizations.

29.10.2008

Nanochemistry UIO

9

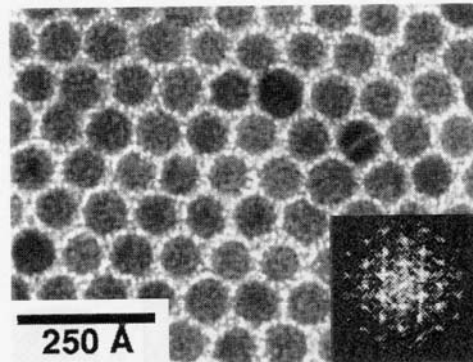
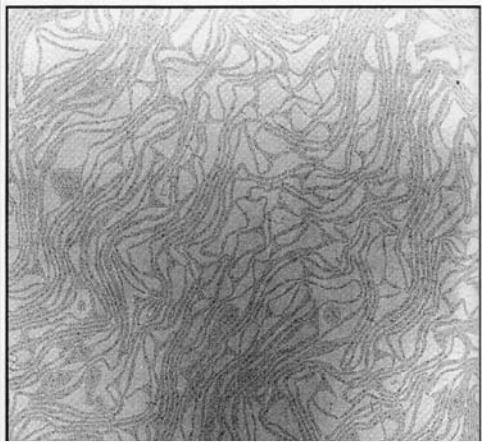


Fig. 4.10. Transmission electron micrograph showing hexagonal close-packed Ag nanocrystals (diameter, 7 nm) obtained by evaporating a chloroform dispersion on a

carbon substrate. The average interparticle distance is 1.5 nm. Inset shows the 2D power spectrum of the image (reproduced with permission from [112]).

# Metal Cluster Organizations

JM

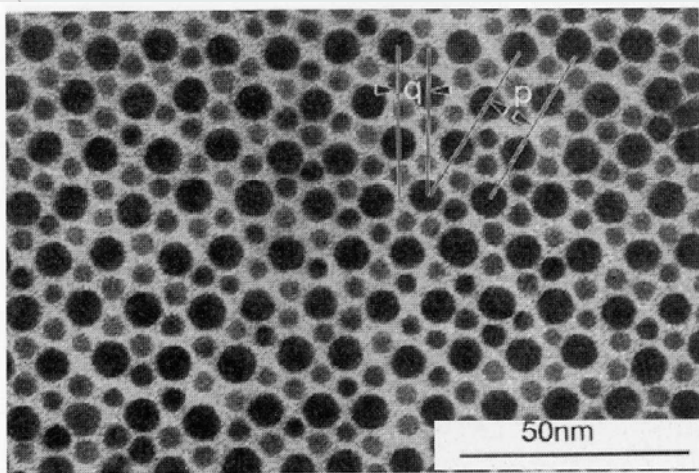


Fig. 4.14. A bimodal hexagonal array of Au nanocrystals. The radius ratio of the nanocrystals is 0.58 (reproduced with permission from [113]).

R. /

29.10.2008

Nanochemistry UIO

10

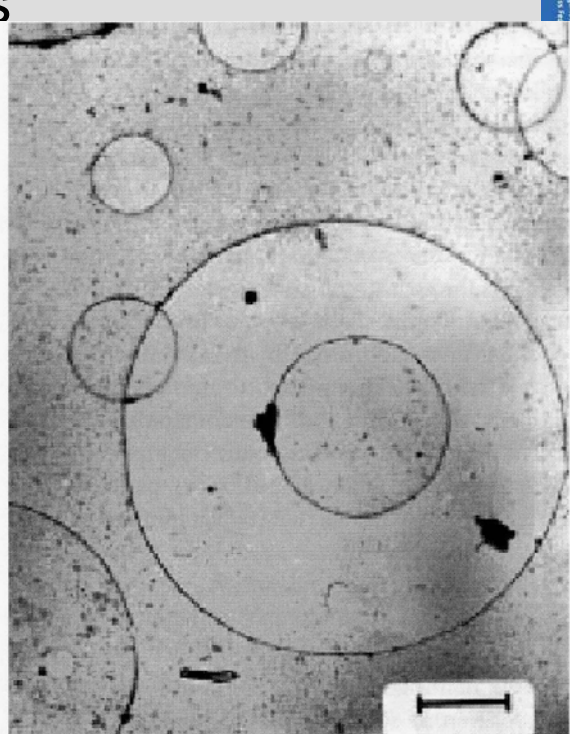
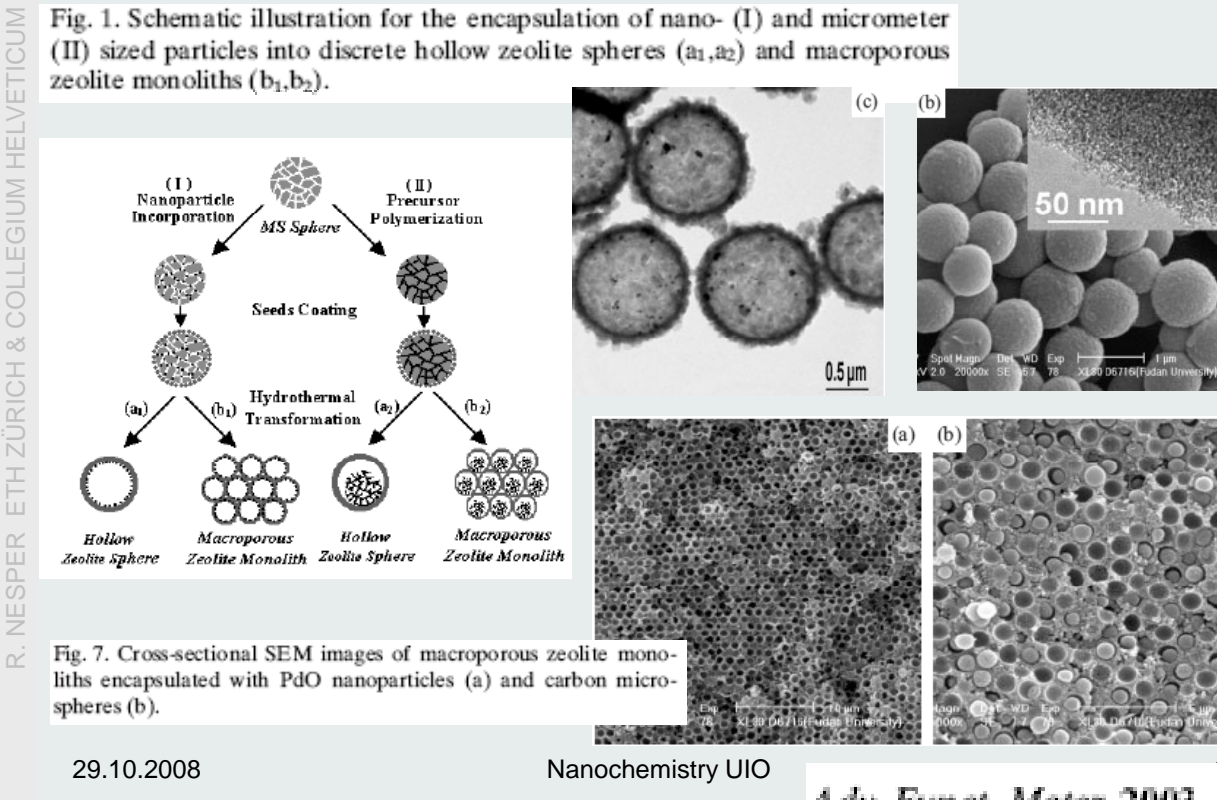
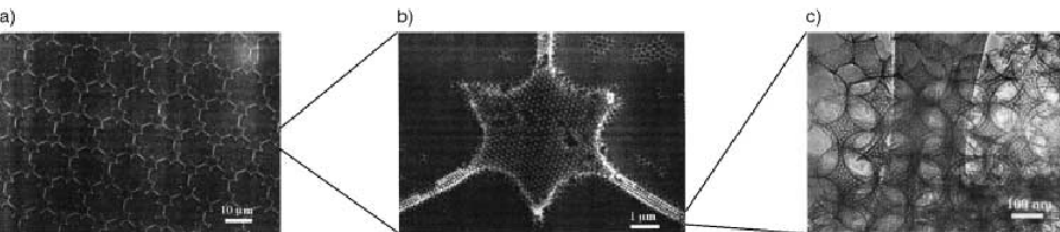
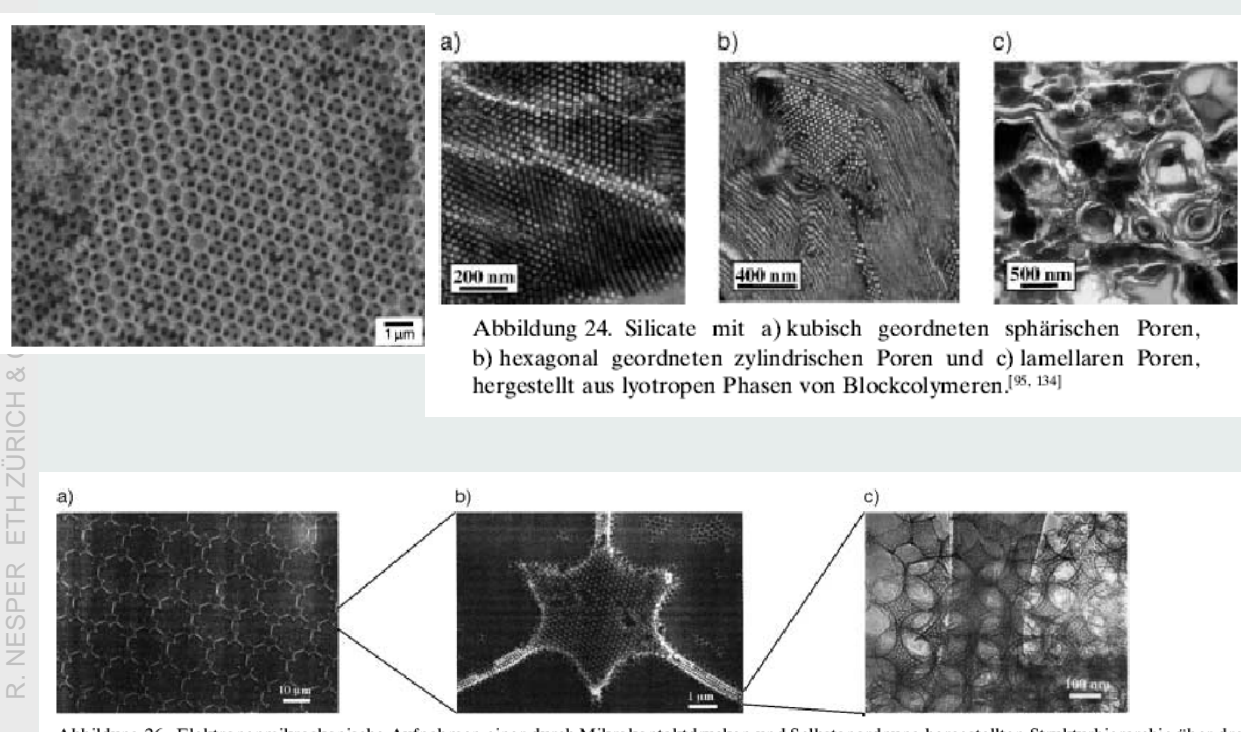


Fig. 6.4. TEM micrograph showing the self-organization of super-paramagnetic nanoparticles into submicron size rings the so-called *Olympic Rings* (scale bar is 0.7 μm).

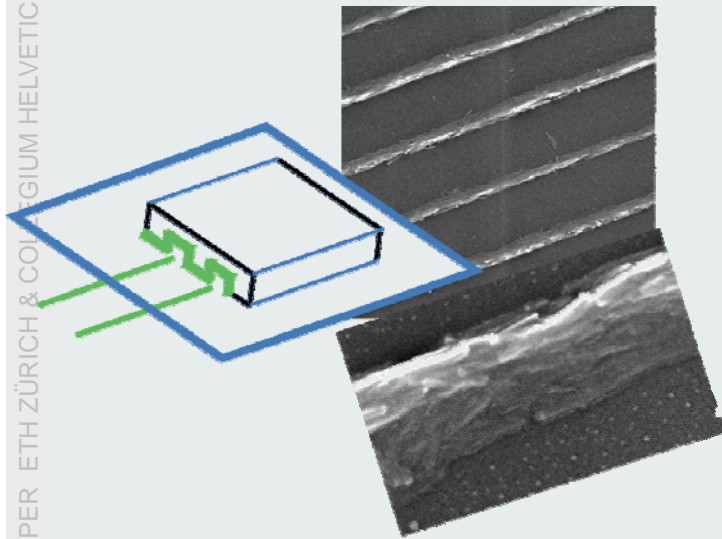
# Hierarchical Crystals from Zeolite Shells



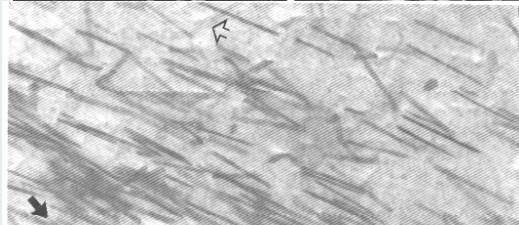
# Selfaggregation and Micro Contact Printing



# Alignment of Nanotubes and Nanorods



collagene +  $\alpha$ -FeOOH composite



J. Webb, D.J. Macey, S. Mann  
in S. Mann, J. Webb, R.J.P. Williams,  
Biomineralization, VCH 1989

H.-J. Muhr, F. Krumeich, U. P. Schönholzer, F. Bieri, M. Niederberger, L. J. Gauckler,  
R. Nesper, *Adv. Mater.* **2000**, *12*, 231-234

29.10.2008

Nanochemistry UIO

13